

On an Experimental Study of the Electron Generation Property of Thin Gold Films

Mehran Vagheian^{1*}, Shahyar Saramad¹, Dariush Rezaie Ochbelagh¹ and Dariush Sardari²

¹Amirkabir University of Technology (Tehran Polytechnic), Tehran, Iran

²Azad University Science and Research Branch, Tehran, Iran

Research Article

Received date: 26/04/2017

Accepted date: 11/05/2017

Published date: 20/05/2017

*For Correspondence

Mehran Vagheian,
Amirkabir University of Technology
(Tehran Polytechnic),
Tehran 14174, Iran.
Tel: +982164540

E-mail: mvagheian@aut.ac.ir

Keywords: Electron generation property,
Thin film characterization, Deposition rate,
Gold films

ABSTRACT

In the present study, the effects of the thickness and deposition rate at different X-ray energies on the electron generation property of thin gold films have been investigated. In order to find out the effects of different thickness, thin gold films with the thickness of 10, 100 and 1000 nanometres at two different deposition rates namely 1 angstrom/s and 1 nm/s have been considered. All the prepared samples have been fabricated using the Physical Vapour Deposition technique (PVD) and characterized by the Energy Dispersive Spectroscopy (EDS), Scanning Electron Microscopy (SEM) and X-Ray Diffraction Technique (XRD). The results all clearly indicate that the yield of electron generation for the deposition rate of 1 angstrom/s is much higher than that those of 1 nm/s. Moreover, the obtained results reveal the superior electron generation property of 100 nm thickness in comparison to the other considered thicknesses.

INTRODUCTION

In recent years, the number of literatures concerning to transmission of various nuclear radiations through nano structured materials has been increased ^[1-10]. Among them, transmission of X-ray through the Nanoparticles has attracted more attention due to its various industrial and medical applications ^[11]. Using of these nano particles mainly is for their wonderful chemical, physical and mechanical properties compared to the conventional micro-sized particles ^[11,12]. Specially, the maximization of surface to volume ratio and the highly efficient dispersion properties of the Nano-sized particles made them attractive for further investigations ^[5,13,14].

A recent study by Noor Azman et al. ^[14] considered the X-ray transmission properties of WO₃ as a filler loading material within the epoxy composites. This research shows a better attenuation ability of nano-sized WO₃ from 25 to 35 keV X-ray energies in compared to the micro-sized WO₃. This research also indicates that the particle size has not a significant role in attenuation properties for the higher X-ray energies (40 to 120 keV). This view is also confirmed by Kunzel and Okuno ^[12] by testing the micro and nano-sized CuO in a polymer resin for different thicknesses and concentrations. This evidence supports the view that the particle size effect emerges mainly in the low energy ranges and it also revealed that the first and perhaps the most important advantage of using the nano particles on the X-ray transmission, is their better dispersion properties within the polymer composites in comparison to micro-sized particles ^[5,11-14].

Another way of viewing on X-ray transmission is to consider the photoelectron generation property. The photoelectric event dominates for X-ray interaction with low energy ranges and high atomic number ^[15,16]. The probability of this event can be significantly depends on particle size. One of the most obvious reasons stems from this fact that the number of particles per gram for the same amount of material, increases with decreasing the particle size ^[11]. As a consequence, the probability of a low energy X-ray photon to be absorbed and generated electrons may be increased.

Since the surface to volume ratio as mentioned before, is considerably increased by decreasing the particle size, so, the escape probability of the ejected electrons will also be increased in nanostructured materials.

Another key factor which can make a significant impact on the electron escape probability is the thickness of the thin film materials [16]. More precisely, by increasing the thickness of the layers, the fraction of deposited energy which can eventually be lead to increase the emission of electrons could be increased. However, it should be noted that by increasing the thickness, the electron capture probability through the medium could also be increased and this issue could consequently impact the total number of recorded electrons. To this end, it seems that investigation around the electron generation property of thin films could be rewarding owing to many applications of X-ray to electron conversion property. Among them, one of the most important applications is for the photomultiplier tubes (PMT), a device which converts the incident light photons into electrons. In PMT, the photocathode serves to convert as many of the incident light photons as possible into low energy electrons [16-18].

The main aim of this study is to determine the electron generation property of thin gold films. Accordingly, in this study, Nano gold particles have been deposited on the substrate using thermal evaporation PVD technique. The experimental implementation has been considered for three different thicknesses namely, 10, 100 and 1000 nanometers. Additionally, the transmission properties of the aforementioned samples have been considered using different X-ray energies. In order to determine the impact of different dispersion properties of the thin film on the X-ray transmission properties, two different deposition rates, namely 1 nm/s and 1 angstrom/s have been used. All the samples were then characterized using the Energy Dispersive Spectroscopy (EDS), Scanning Electron Microscope (SEM) and also X-ray Diffraction Technique (XRD).

EXPERIMENTAL PROCEDURE

Sample Preparation

As thin gold films have a number of different applications in many important fields of science and technology such as conductive application, radiation therapy, x-ray imaging technology and radiation detection, some methods of fabrications have been introduced in the literature. All of the techniques almost need a substrate for deposition purpose and in most of the cases the substrate could itself has an influence on the results of study phenomenon. In this work, to reduce the impact of the substrate on the measurement of irradiation, some significant parameters such as the thickness and constructions of the substrate structure (such as the atomic numbers) in addition to the desirable geometry for the experiments has been considered. After evaluation of the aforementioned factors and consideration of the candidates, the standard borosilicate-thin coverslips with the thickness of about 130 μm are used. Then, the gold nanoparticles are deposited on the substrate with different deposition rates (i.e., 1 nm/s and 1 angstrom/s) and thicknesses (i.e., 10, 100 and 1000 nanometers) using the PVD technique (Varian model V70).

Characterization

At first, the EDS technique has been employed to exactly determine the purity of the gold material. Second, the SEM (KYKY model EM 3200) images have been employed to distinguish the surface morphology and uniformity of the coated layers which are significantly depends on the thicknesses and deposition rates. Furthermore, in order to study the characterization of the prepared samples, the XRD technique (INEL model EQUINOX 3000) has been used.

RESULTS AND DISCUSSION

Energy Dispersive X-ray Spectroscopy Analysis

In order to prevent undesirable impurities which can significantly be contributed in the measurements, a high pure Swiss made gold (Produits Artistiques Metaux Precieux) has been used. **Figure 1** shows the EDS spectra of the samples (ZAF software) with 9.440 kV voltages.

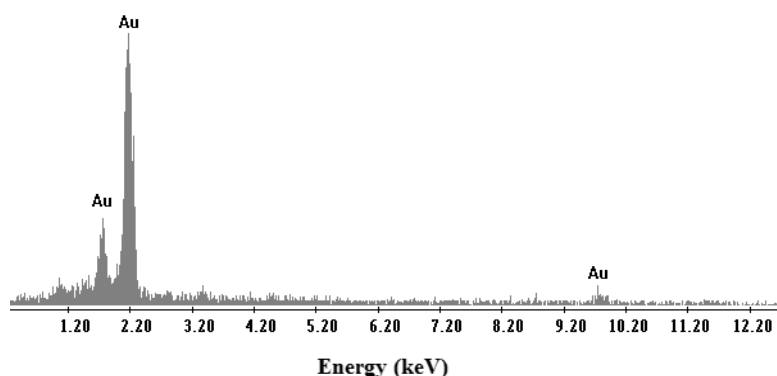


Figure 1. EDS spectrum of gold nanoparticles.

As is observable, the presence of gold in the EDS spectra is shown while there is no evidence for any undesirable impurities.

Scanning Electron Microscopy Observations

First of all, the SEM technique is used to determine the thickness of the deposited thin films. This analysis is accomplished for the sample of 100 and 1000 nanometer thickness with both the deposition rates. **Figures 2 and 3** show the cross face of deposit thin gold films on the substrate. For facilitating comparison between the aforementioned techniques, it can be observed that the thickness measured by the SEM technique is in good agreement with the thickness which were evaluated by the PVD technique. To consider the surface morphology of the deposited gold thin films, the SEM technique is employed. **Figure 4** shows the surface morphology of the coated gold films for different thicknesses (i.e., 10, 100 and 1000 nm) and deposition rates (i.e., 1 angstrom/s and 1 nm/s). The first thing that could be seen from this figure is the relation between the surface morphology with the thickness of the coated thin films. More precisely, the deposited Nano particles seem to be agglomerated as the thickness is increased for each deposition rate. Form different point of view, it is also observable for the same thicknesses that; the uniformity of distributed particles on the substrate for the deposition rate of 1 angstrom/s is much better than those of 1 nm/s. To be more precise, Nano gold particles could be distributed more uniformly throughout the substrate by reducing the deposition rate from 1 nm/s to 1 angstrom/s. As is mentioned in the introduction section, this feature is very important to maintain or enhance the electron generation property of the materials.

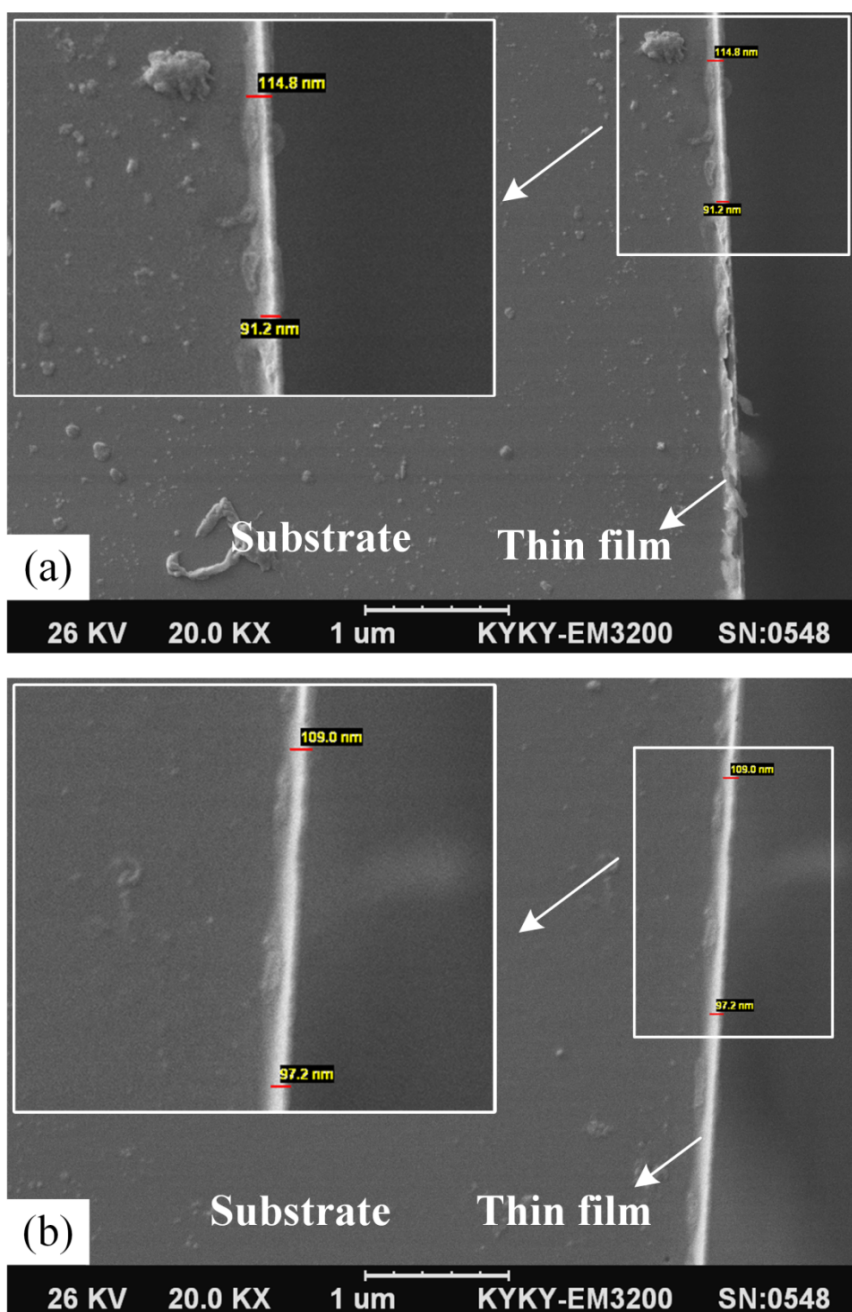


Figure 2. SEM images of (a) 10 nm thickness of gold with 1 angstrom/s deposition rate, (b) 10 nm thickness of gold with 1 nm/s deposition rate.

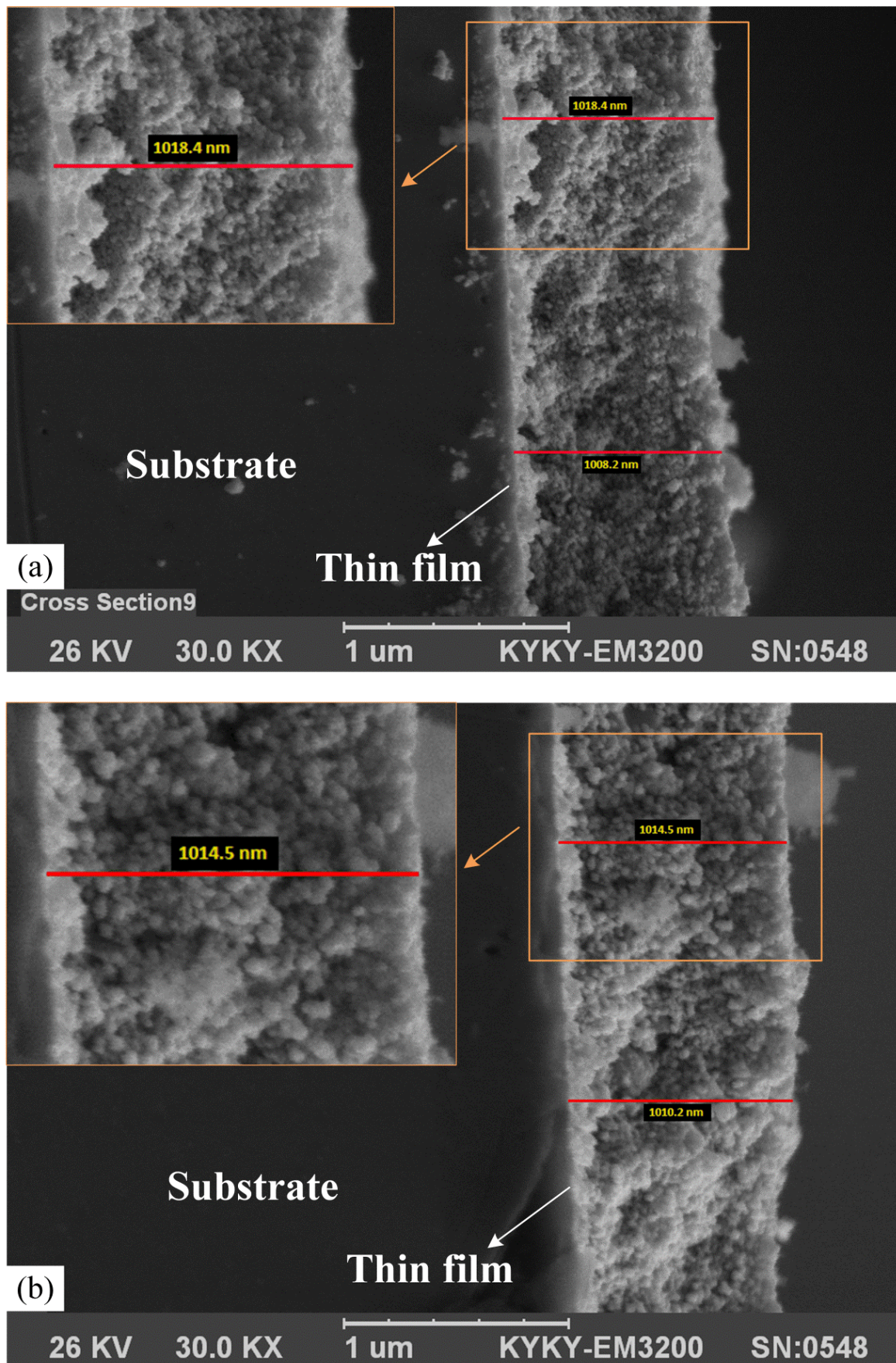


Figure 3. SEM images of (a) 1000 nm thickness of gold with 1 angstrom/s deposition rate, (b) 1000 nm thickness of gold with 1 nm/s deposition rate.

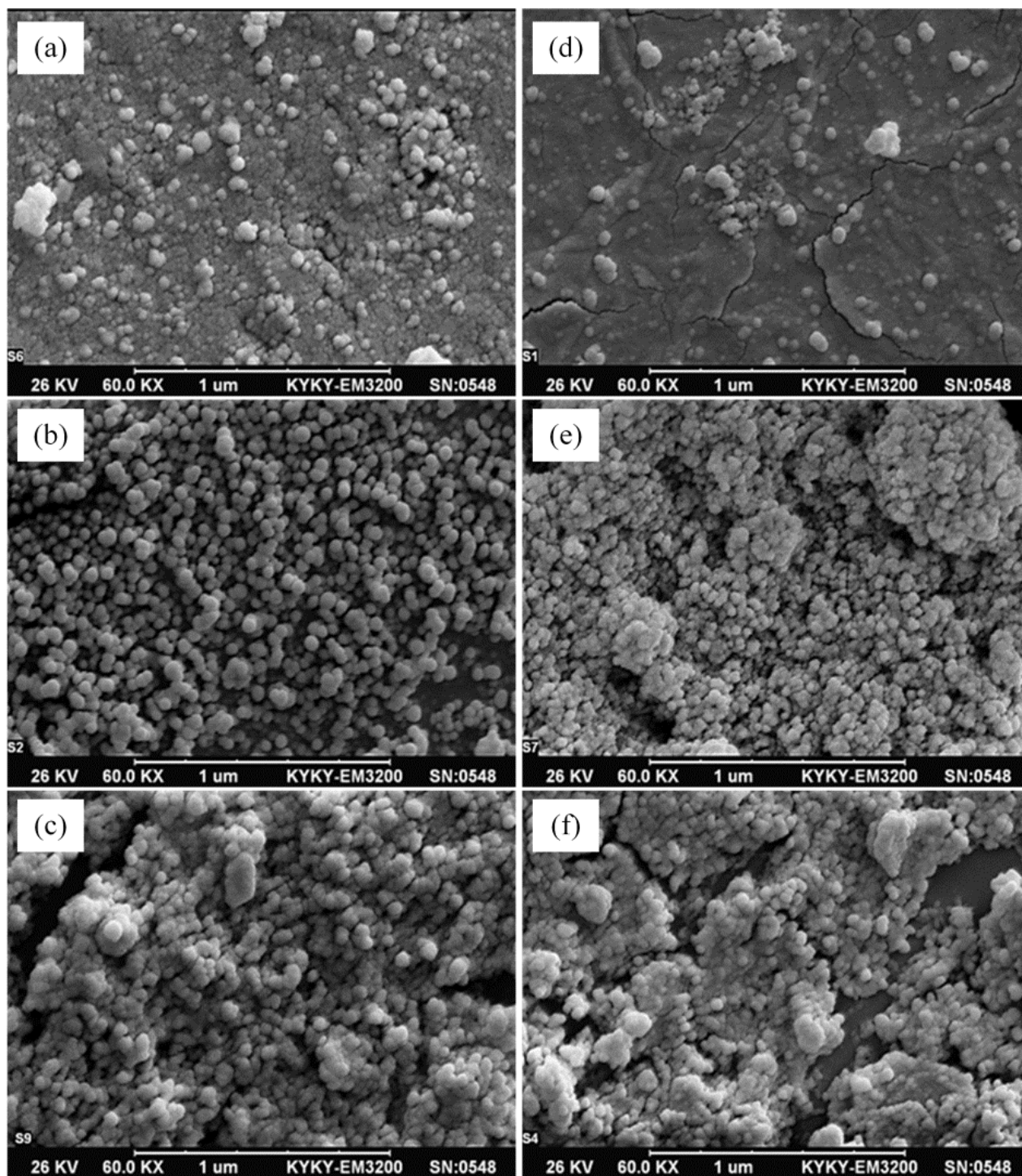


Figure 4. SEM images of (a) 10 nm thickness of gold with 1 angstrom/s deposition rate, (b) 100 nm thickness of gold with 1 angstrom/s deposition rate, (c) 1000 nm thickness of gold with 1 angstrom/s deposition rate, (d) 10 nm thickness of gold with 1 nm/s deposition rate, (e) 100 nm thickness of gold with 1 nm/s deposition rate and (f) 1000 nm thickness of gold with 1 nm/s deposition rate.

X-ray Diffraction Pattern Analysis

The phase structure of all samples has been characterized using a typical XRD which operates at 40 kV and 30 mA tube voltage and current, respectively. The source of the equipment was copper $\text{K}\alpha$ with the wavelength of 1.541 Å. Moreover, it is interesting to note that all of diffraction peaks have been illustrated in the 2θ range of -10.469° to 120.347° with a step size of 0.032° . **Figure 5** shows one diffraction peak at 5.654° for the substrate, which reveals that the substrate is an amorphous structural material. Moreover, **Figure 6** gives evidence for the presence of the deposited gold material due to the obtained diffraction peaks. According to the measured results, the main diffraction peaks appear at 38.224° , 44.490° , 64.784° , 77.205° , 81.359° , 97.721° , 110.483° and 115.273° attributed to the reflection plans of (111), (200), (220), (311), (222), (400), (331) and (420), respectively (JCPDS card no. 004-0784). This figure also confirms the absence of impurities in the samples which is in agreement with the EDS analysis as in **Figures 1 and 6**.

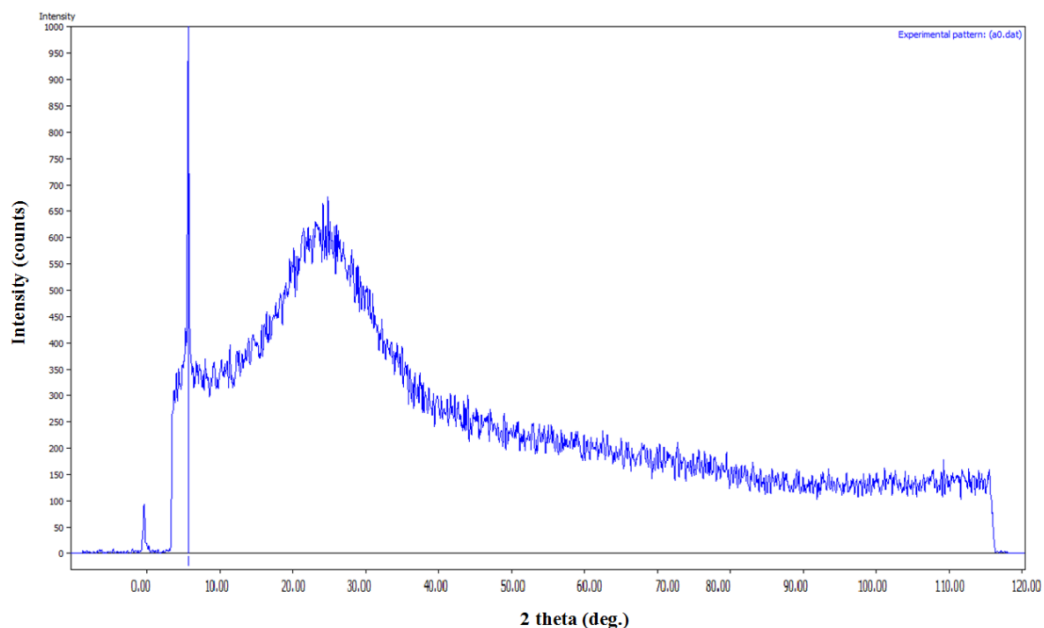


Figure 5. X-ray diffraction pattern of the thin glass slide.

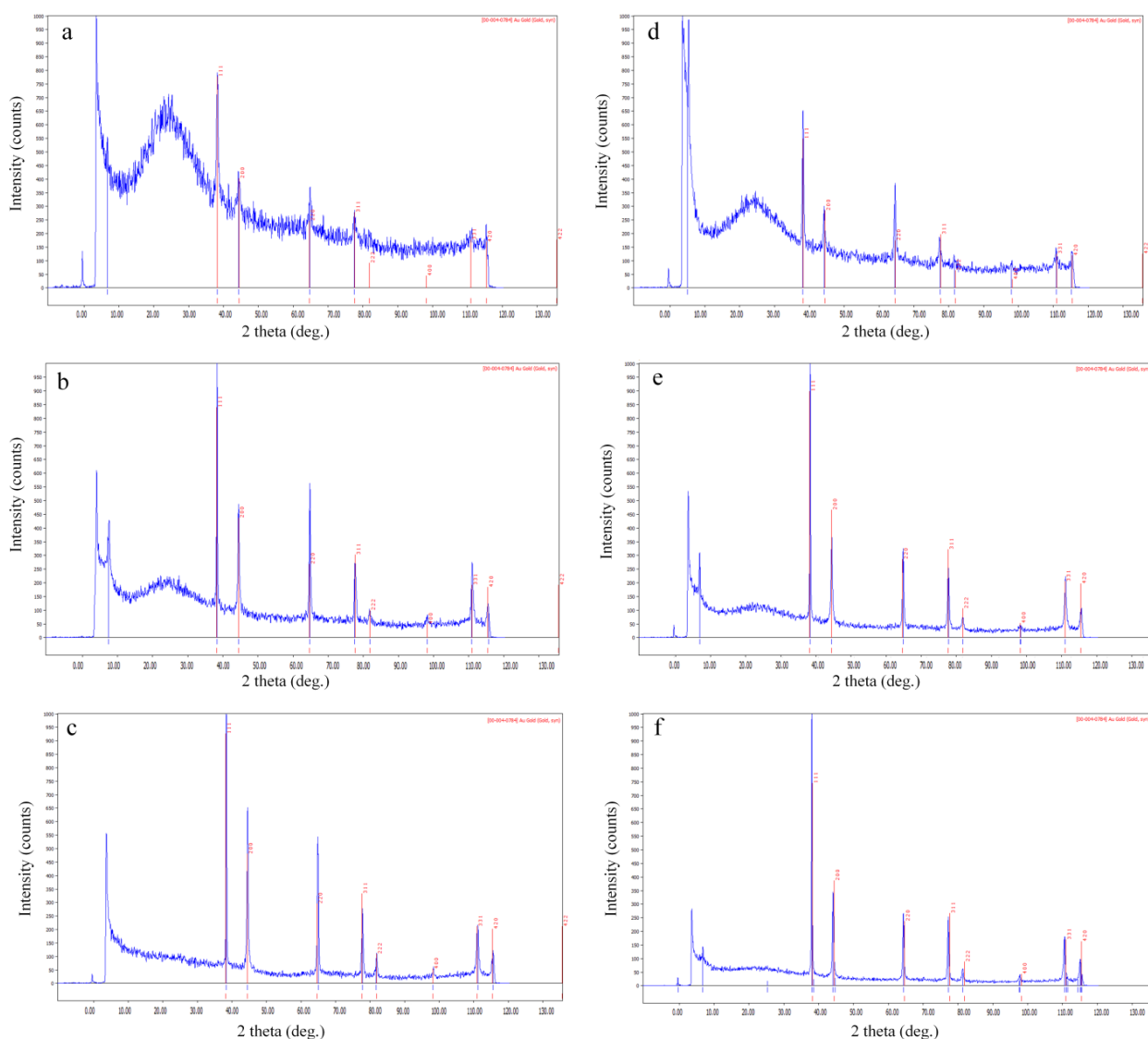


Figure 6. X-ray diffraction patterns of (a) 10 nm thickness of gold with 1 angstrom/s deposition rate, (b) 100 nm thickness of gold with 1 nm/s deposition rate, (c) 1000 nm thickness of gold with 1 angstrom/s deposition rate, (d) 10 nm thickness of gold with 1 nm/s deposition rate, (e) 100 nm thickness of gold with 1 nm/s deposition rate and (f) 1000 nm thickness of gold with 1 nm/s deposition rate.

The averaged grain size of the deposited gold Nano particles has been extracted using the Williamson-Hall (W-H) method. This method is based on the principle that the approximate formula for sizing broadening, and strain broadening, vary quite differently with respect to Bragg angle, θ . More precisely, this classical method can obtain quantitative information about the grain size using the assumption that both size and strain broadened profiles are Lorentzian. So, a mathematical relation could be established between the integral breadth, volume weighted average domain size and the strain. Where, size-strain parameters can be obtained from the “size-strain plot” (SSP). This has the benefit that less importance is given to data from reflections at high angles^[19-22]. According to this technique, the particle size can be calculated from the slope linearly fitted data. The average gold Nano particle crystalline sizes are equal to 15 nm, 32.45 nm, 30.60 nm, 31.54 nm, 32.58 nm and 35.71 nm for the samples a, b, c, d, e and f, respectively. As it is apparent, the grain size of the prepared samples with 1 angstrom/s deposition rate is smaller than the sample with 1 nm/s deposition rate.

X-ray Irradiation

In order to characterize the electron generation property of the fabricated thin gold films, a typical X-ray tube (PHYWE RONTGENDERAT) with a copper target and a maximum 23 kV tube voltage has been used. Additionally, a Geiger Mueller counter has been employed to count the number of transmitted radiations. In this part of work, six samples which are prepared based on the previous sections, are located between the X-ray tube and the detector. Moreover, it should be noted that each sample were analyzed by energy ranged from 18 keV to 23 keV. In the experimental setup the X-ray beam incidents initially to the substrate prior the thin gold films^[16,23]. Note, the attenuation of glass slide for the used X-ray energies in this work is less than 2%. Regarding the electron generation event, the ratio of the total number of photons as well as electrons extracted from the surface of thin gold films to the number of photons entering the thin gold films have been studied. As it is shown in **Figure 7**, this quantity which has been called the magnification factor (M) is depicted versus thickness of the thin gold films at different X-ray energy. Based on the definition of magnification factor, one could formulate this parameter as follows:

$$M = \frac{I_{electron} + I_{photon}}{I_{photon}} \tag{1}$$

where, $I_{electron}$ and I_{photon} are the electron and photon intensity, respectively. By considering this equation, it will be clear that the number of the generated electrons through the gold thin films can increase the value of this parameter (M) above 1.

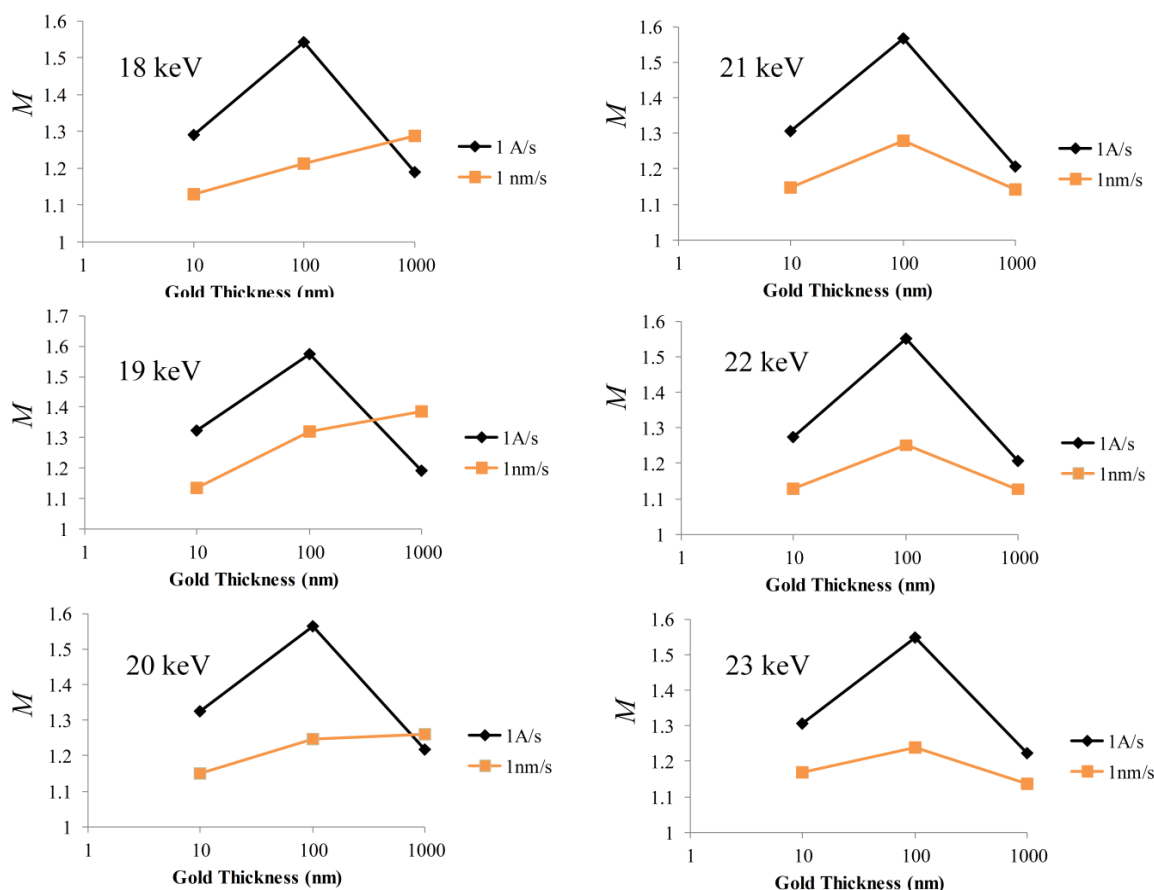


Figure 7. The measured magnification factor (M) versus different thickness of thin gold films (i.e., 10, 100 and 1000 nm/s) by considering different deposition rate (i.e., 1 angstrom/s and 1 nm/s) and impinging X-ray energy (i.e., 18, 19, 20, 21, 22 and 23 keV).

The first outcome that will be clear from **Figure 7** is increasing the magnification factor from 10 to 100 nanometers for all X-ray energies and deposition rates. This may be due to the fact that the fraction of deposition X-ray energies increases with increasing the thickness of gold layers which can eventually be led to more photoelectron generation probability. However, for the both deposition rates, the magnification factor is decreased when thickness increases to 1000 nanometers. This fact is laid upon the fact that the range of the generated electrons is comparable to this thickness of gold film (1000 nm).

According to the results illustrated in **Figure 7**, it is possible to observe the effect of different deposition rates on the electron generations. As can be seen, for all X-ray energies the magnification factor for the deposition rate of 1 angstrom/s is higher than 1 nm/s for 10 and 100 nanometer thicknesses. However, the variations with the X-ray energies are noticeable for the sample of 1000 nanometers. Perhaps the main reason for these results can be explained regarding **Figure 4** where the uniformity of the samples of 1 angstrom/s deposition rate for all thicknesses is substantially more than the other ones. This can likely be led to more escaping probability of the generated electrons through the medium. Based on these analysis, it may be inferred that, the aforementioned reason can be logical for 10 and 100 nanometer thicknesses. Though, in the case of 1000 nanometer thickness, the limitation ranges of the generated electrons seem to be dominant for lower X-ray energies as compared to ones which generated from higher energies.

Based on the arguments cited above, the electron generation event can considerably impact on the number of extracted radiations from the surface of thin films. However, by considering the fact that only one signal can be produced by the detector for the impinged photons as well as electrons, so no significant changes should be observed even by generating additional electrons through the medium. The most obvious explanation for this might be from the point of view of comparative timing events. More precisely, the generated electrons need more time to reach the detector in comparison with the transmitted photons. So, these electrons can contribute to producing additional signals. Accordingly, by increasing the generated electrons, the recorded signals can eventually be increased (see **Figure 7**). To elaborate on this issue, one more experiment has been carried out. Based on this experiment, a bare cover slip was firstly located near the X-ray tube and then near the Geiger-Muller counter. In the next step, this experiment has been replicated by using the sample of 1000 nanometer thickness with 1 angstrom/s deposition rate. The implementation of this experiment has been considered for different X-ray energies and for both cases. The results all showed that changing the location of the cover slip (the first case) at different distances does not have any impacts on the measurements. However, the results for the second sample (i.e., the 1000 nanometer thickness) showed that the counting ratio significantly differed by changing the location of the irradiated sample between the source and the counter. In other words, by closing the sample to the counter for the second sample, the recorded radiations were increased. This implies that the generated electrons have strength to reach the counter when the sample is near the Geiger-Muller. On the other hand, because almost no significant electrons generated in the bare substrate, almost no differences will be appeared in the measurements by changing the location of the first sample between the distance of X-ray tube and the Geiger-Muller counter.

CONCLUSION

This paper aims to clarify the effect of different thickness, deposition rate and X-ray energy on the electron generation property of thin gold films. Accordingly, the effect of different thickness has been considered by fabricating thin films with the thickness of 10, 100 and 1000 nanometer, and the effect of deposition rate has been considered by fabricating the samples for different deposition rates of 1 nm/s and 1 angstrom/s.

All the samples have been prepared by using the Physical Vapor Deposition technique (PVD) and characterized by the Energy Dispersive Spectroscopy (EDS), Scanning Electron Microscope (SEM) and X-Ray Diffraction Technique (XRD). The results all showed the superior electron generation property of 1 angstrom/s deposition rate than those for 1 nm/s. Moreover, the results indicate that the electron generation yield of 100 nm thickness was much greater than the other thicknesses. It also has been demonstrated that the energy of incident photons has negligible impacts on the results for the sample with 1000 nm gold thickness due to the comparable electron energy ranges with the mentioned thickness. According to the satisfactory results reported herein, it looks very promising for future application of the thin gold films to employ as an efficient structure for converting photons to electrons.

Highlights:

- Different thickness of thin gold films has been fabricated using the Physical Vapor Deposition technique (PVD).
- The samples have been prepared at two different deposition rates, namely 1 angstrom/s and 1 nm/s.
- The effects of thickness and deposition rate at different X-ray energies on the electron generation property of thin gold films have been investigated.

The results all indicated variation of the electron generation yield based on the variation of different factors.

REFERENCES

1. Sohrabnezhad Sh, et al. Gamma ray effects on optical properties of CoS nanoparticles. Spectrochim Acta A. 2012; 96:796-800.

2. Adliene D, et al. Low energy X-ray radiation impact on coated Si constructions. *Radiat Phys Chem.* 2010;10:1031-1038.
3. Deguedre C and Veleva L. Electron energy loss spectroscopy investigations through nano-ablated actinide dioxide samples. *Prog Nucl Energy.* 2014;72:96-100.
4. Nakamura T, et al. Overview of recent experimental works on high energy neutron shielding. *Prog Nucl Energy.* 2004;2:85-187.
5. Noor Azman NZ, et al. Synthesis and Characterization of ion-implanted epoxy composites for X-ray shielding. *Nucl Instrum Methods Phys Res Sec B.* 2012;15:120-123.
6. Artem'ev VA. Estimate of neutron attenuation and moderation by nanostructural materials. *Atom Energy.* 2003;4:327-330.
7. Kim J, et al. Enhancement of thermal neutron attenuation of nano-B₄C, -BN dispersed neutron shielding polymer nanocomposites. *J Nucl Mater.* 2014;3:48-53.
8. Kim J, et al. Particle size-dependent pulverization of B₄C and generation of B₄C/STS nanoparticles used for neutron absorbing composites. *Nucl Eng Technol.* 2014;5:675-680.
9. Kim J, et al. Dispersed gamma radiation shielding materials. *Adv Eng Mater.* 2014;9:1083-1089.
10. Hosseini SH, et al. Synthesis, characterization and X-ray shielding properties of polypyrrole/lead nanocomposites. *Polym Advan Technol.* 2015;6:561-568.
11. Botelho MZ, et al. X-ray transmission through nanostructured and microstructured CuO materials. *Appl Radiat Isot.* 2011;2:527-530.
12. Kunzel R and Okuno E. Effect of the particle sizes and concentrations on the X-ray absorption by CuO compounds. *Appl Radiat Isot.* 2012;4:781-784.
13. Noor Azman NZ, et al. Characterization of micro-sized and nano-sized tungsten oxide-epoxy composites for radiation shielding of diagnosis X-rays. *Mat Sci Eng C.* 2013;8:4952-4957.
14. Noor Azman NZ, et al. Effect of particle size, filler loadings and x-ray tube voltage on the transmitted x-ray transmission in tungsten oxide-epoxy composites. *Appl Radiat Isot.* 2013;1:62-67.
15. Meyerhof WE. *Elements of nuclear physics.* McGraw-Hill, The United States. 1967.
16. Knoll GF. *Radiation detection and measurement.* The United States (NY): John Wiley and Sons, Inc.; 2000.
17. Gontad F, et al. Growth of poly-crystalline Cu films on Y substrates by picosecond pulsed laser deposition for photocathode applications. *Nucl Instrum Meth A.* 2015;799:70-74.
18. Sumiya M, et al. Fabrication and hard X-ray photoemission analysis of photocathodes with sharp solar-blind sensitivity using AlGa_N films grown on Si substrates. *Appl Surf Sci.* 2012;14:4442-4446.
19. Prabhu YT, et al. X-ray analysis of Fe doped ZnO nanoparticles by Williamson-Hall and size-strain plot. *IJEAT.* 2013;1:268-274.
20. Prabhu YT, et al. X-ray analysis by Williamson-Hall and size-strain plot methods of ZnO nanoparticles with fuel variation. *WJNSE.* 2014;1:21-28.
21. Sivakami R, et al. Estimation of lattice strain in nanocrystalline RuO₂ by Williamson-Hall and size-strain plot methods. *Spectrochim Acta A.* 2015;5:43-50.
22. Venkateswarlu K, et al. X-ray peak broadening studies of nanocrystalline hydroxyapatite by Williamson-Hall analysis. *Physica B.* 2010;20:4256-4261.
23. Baishali G, et al. Study of electron focusing in thick GEM based photon detectors using semitransparent photocathodes. *Nucl Instrum Methods Phys Res Sec A* 2013;21:51-57.